Fine Structures of Curved Edge-On Lamellae in Crystalline Thin Films of Isotactic Polystyrene As Revealed by Transmission Electron Microscopy

Masaki Tsuji,* Masahiro Fujita,† Toshiki Shimizu,‡ and Shinzo Kohjiya

Laboratory of Polymer Condensed States, Division of States and Structures III, Institute for Chemical Research, Kyoto University, Uji, Kyoto-Fu 611-0011, Japan

Received February 5, 2001; Revised Manuscript Received April 13, 2001

ABSTRACT: Amorphous thin films of isotactic polystyrene (i-PS) were prepared by casting a hot solution in *p*-xylene onto the hot water surface. Dried films mounted on the specimen grids for transmission electron microscopy (TEM) were crystallized from the glassy state by annealing. The crystalline thin films of i-PS thus prepared were examined by TEM. In these films, we could observe immature and more or less mature two-dimensional spherulites and sheaflike structures, the constituents of which are basically edge-on lamellae. As for the space-filling mechanisms of spherulitic growth, some models have been proposed so far: for example, a model based on branching of straight lamellae and a model based on "spawning" of new lamellar crystals. In the latter model, however, most of the spawned lamellae are to be curved. From TEM observations, it is deduced that both branching and spawning occur together in the process of spherulitic growth of i-PS, because some lamellae are seemingly straight and branched but the majority of lamellae are curved. In addition, the (300) lattice images obtained by high-resolution TEM have successfully visualized, at the molecular level resolution, the two manners for producing such curved lamellar crystals with an edge-on orientation in crystalline thin films of i-PS.

1. Introduction

Extensive studies on solid structure and properties of isotactic polystyrene (i-PS) have been reported so far concerning crystallization from solution,[1−7] from the glassy state,[8−11] or from the melt[6,8,12−14] because of, for example, the small growth rate of i-PS in crystallization. The crystal of i-PS is vulnerable to electron irradiation similar to other polymer crystals, so that the crystal becomes amorphous by a small irradiation dose. The i-PS crystal is, however, several times more durable than, for example, that of polyethylene against electron irradiation.[3,4,9] By using a transmission electron microscope equipped with a special device to minimize the radiation damage such as a minimum dose system (MDS; JEOL Ltd.) or a low dose unit (LDU; Philips), therefore, direct lattice imaging of i-PS crystals has been successfully carried out so far even at room temperature.[3,4,9]

As for the homogeneously nucleated polymer spherulite, a structural model, in which straight ribbonlike lamellar crystals branch repeatedly for space filling, was previously proposed (for example, refs 15 and 16). Subsequently, a different model, in which ribbonlike lamellae are nucleated one after another during spherulitic growth and then they are curved and splayed (or fanned) as they grow, was also proposed (for example, refs 17−19). In this report, crystalline thin films of i-PS are investigated by transmission electron microscopy (TEM), in particular by high-resolution TEM (HRTEM). Some important fine structural results obtained from the edge-on lamellae of i-PS, which are constituents of two-dimensional spherulites and of sheaflike structures, are described. The space-filling mechanism for the spherulites is also briefly discussed on the basis of morphological observations by TEM.

2. Experimental Section

2.1. Sample Preparation. The i-PS sample (Polymer Laboratories Ltd.; the molecular weight reported by the supplier is approximately 6×10^5) was dissolved in hot *p*-xylene (near its boiling point), and a drop of the resultant hot solution (1−2 wt %) was spread on the surface of hot water (near but below the boiling point of water) to make a thin amorphous film of i-PS because the temperature of hot water is near or below the glass transition temperature of i-PS (90−100 °C).[8,10] The thickness of the film was around 100 nm or less as judged from its interference color (silver to light gold). This is the same method as that used to make thin films of polyethylene and isotactic polypropylene with spherulitic textures.[20] The amorphous thin film of i-PS was mounted onto a specimen grid (Cu) for TEM (or onto a microgrid[21] deposited on a Cu grid for HRTEM) and then annealed/crystallized isothermally at 160−170 °C under a nitrogen atmosphere for a given time (usually about 10 min). This process is the case of so-called "cold crystallization", namely, of crystallization from the "glassy state".[22−24] After annealing/crystallization, the specimens were coated and reinforced only with a thin carbon layer vapor-deposited under vacuum. To enhance the morphological contrast in conventional bright-field imaging by TEM, some specimens were shadowed with Pt−Pd under vacuum at a shadowing angle of $\tan^{-1}(1/4)$ before carbon coating. For calibration of camera length in selected-area electron diffraction (SAED), some of the specimens were coated under vacuum with Au instead of Pt−Pd.

2.2. Transmission Electron Microscopy (TEM). The present TEM study was performed at room temperature by using a JEOL JEM-200CS (accelerating voltage = 200 kV; spherical aberration coefficient (C_s) = 2.8 mm) or a JEOL JEM-2010 (200 kV; C_s = 0.5 mm), both of which are equipped with a MDS. The SAED patterns and the TEM images were recorded onto photographic films (Fuji FG, Kodak SO-163 or

† Research Fellow (1998−2001) of the Japan Society for the Promotion of Science.

‡ Toyo Tire & Rubber Co. Ltd., 5-7, Nishichujo, Ibaraki, Osaka-Fu 567-0887, Japan.

* To whom all correspondence should be addressed. Tel +81-774-38-3061; Fax +81-774-38-3069; E-mail tsujimas@scl.kyoto-u.ac.jp.

10.1021/ma010203n CCC: $20.00
Published on Web 06/02/2001

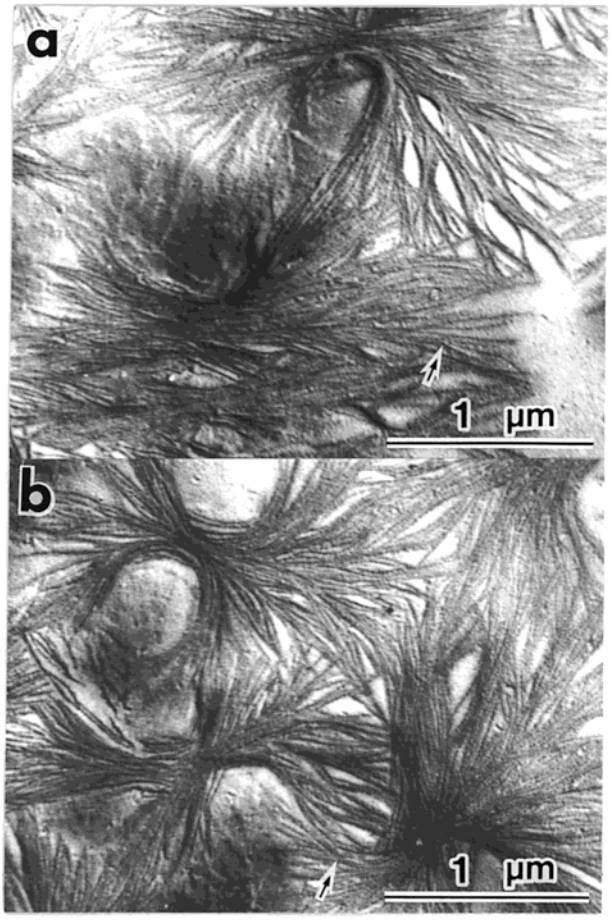

Figure 1. Conventional bright-field images of an i-PS thin film which was crystallized at 165 °C for 10 min and then shadowed with Pt−Pd. The arrow in each image indicates an example of lamellar branching.

Mitsubishi MEM): The characteristics of these photographic films have been reported before.[25,26] The exposed films were developed at 20 °C with a Mitsubishi Gekkol developer (full strength) usually for 5 min. HRTEM images, however, were recorded onto the MEM films and developed at 20 °C with Gekkol for 10 min.

3. Results and Discussion

3.1. Morphological Observations. Parts a and b of Figure 1 are conventional bright-field images of an i-PS thin film annealed/crystallized at 165 °C for 10 min, corresponding to an early stage of spherulitic growth (the specimen was shadowed with Pt−Pd). Owing to the metal shadowing, in these figures, the individual fibrillar entities comprising a more or less mature two-dimensional spherulite with a central "binocular-like" open space (such a spherulite is located at the upper left of Figure 1b) are well recognized. A so-called sheaflike structure is also visible at the lower left of Figure 1a. As demonstrated below (Figures 2−4), these fibrillar entities are the crystalline lamellae in the "edge-on" position. Some fibrillar entities are seemingly straight, but fibrillar ones surrounding the binocular-like open space are curved. The arrow in Figure 1a,b indicates an example of lamellar branching.

Figure 2 is a bright-field image of an i-PS thin film annealed/crystallized at 170 °C for about 60 min, but this specimen film was not treated by shadow casting[27] or by electron staining.[27] As demonstrated below (see Figure 3), this specimen film is semicrystalline, and

Figure 2. Bright-field image of an i-PS thin film which was crystallized at 170 °C for about 60 min. This image was obtained by the defocus contrast method,[28] namely, taken at a fairly large amount of objective-lens defocus (at an under-focus of about 40 μm at 200 kV).

each of the dark fibrillar striations corresponds to an edge-on lamella. The image in Figure 2 was obtained by the objective-lens defocus contrast method, using an under-focus of about 40 μm at 200 kV. This technique was first introduced by Petermann and Gleiter.[28] For such a semicrystalline specimen which consists of crystalline entities and their amorphous surroundings, a proper amount of objective-lens defocus in the bright-field imaging mode gives sufficient "phase contrast" to the image, owing to the difference in electrostatic inner potential. In Figure 2, sheaflike structures are recognized here and there, and dark fibrillar striations comprised of the edge-on lamellae are clearly observed to be stacked closely near the center of each sheaflike structure. Fibrillar striations near the center of a sheaflike structure are seemingly straight, but those surrounding the binocular-like open space are certainly curved, as in Figure 1. Branched dark striations are also recognized here and there in Figure 2, suggesting lamellar branching.

Figure 3a is also a bright-field defocus-contrast image (taken at an under-focus of about 40 μm at 200 kV) of an i-PS thin film annealed/crystallized at 161 °C for 7 min (the specimen film was not metal-shadowed or stained). In the corresponding SAED pattern (Figure 3b), some crystalline reflections are visible as schematically indicated in Figure 3c, showing that the specimen film is semicrystalline. Gray regions between the dark fibrillar striations represent amorphous regions. Similar to Figure 2, edge-on lamellae are observable as dark fibrillar striations, and stacked lamellar structures are

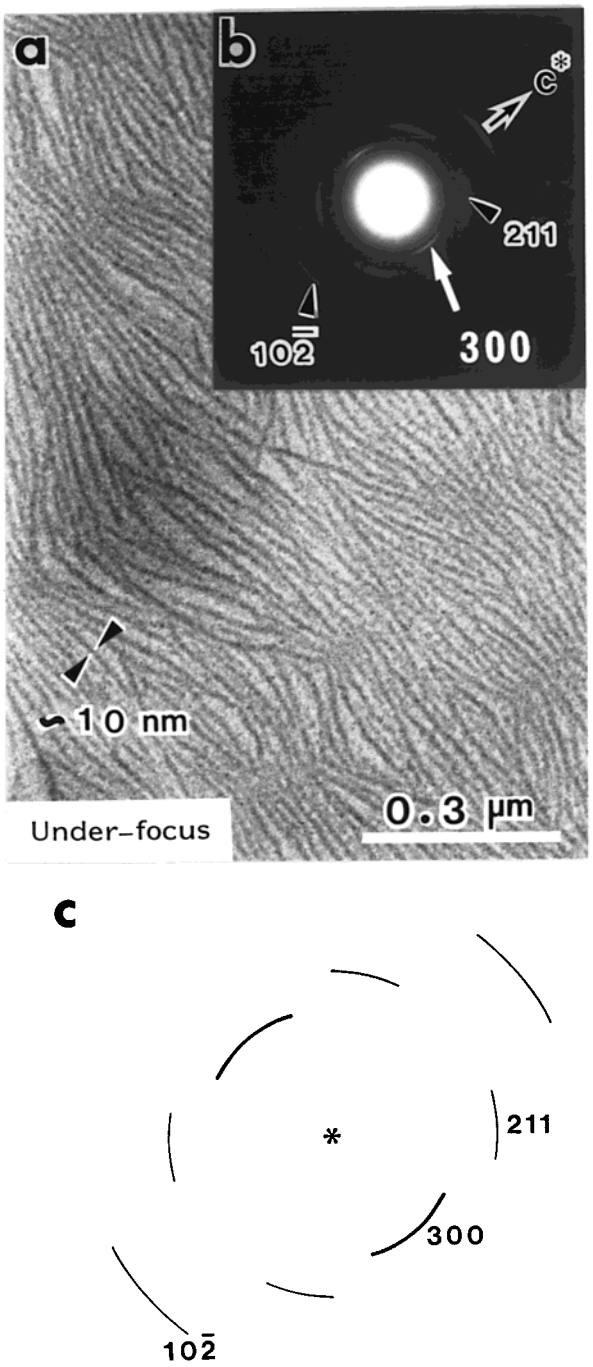

Figure 3. Slightly oriented thin film of i-PS which was crystallized at 161 °C for 7 min. (a) Bright-field image obtained by the defocus contrast method,[28] namely, taken at a fairly large amount of objective-lens defocus (at an under-focus of about 40 μm at 200 kV). (b) Corresponding SAED pattern. (c) Schematic illustration of the SAED pattern shown in (b). The arc-shaped 300 reflection is much sharper and stronger than the others (211 and $10\bar{2}$), as observed in (b). The asterisk (*) indicates the center of the pattern in (c).

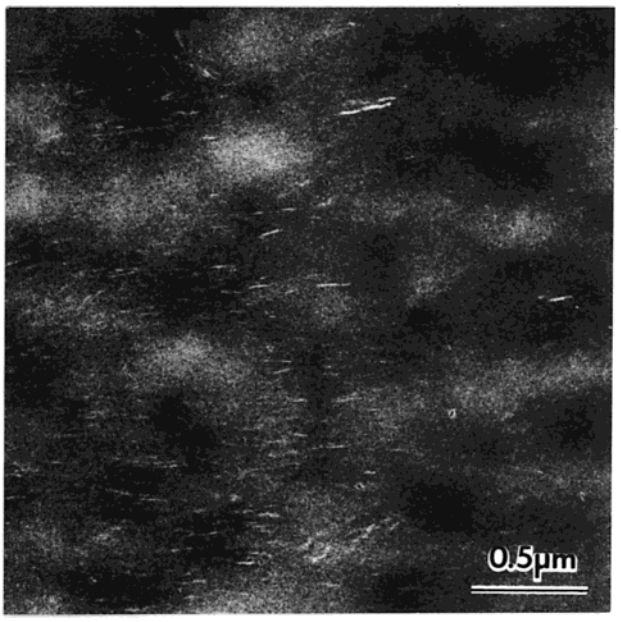

Figure 4. Dark-field image of a slightly oriented thin film of i-PS which was crystallized at 161 °C for 7 min. This image was taken by using one of a pair of the arc-shaped 300 reflections which appeared on the equator in the corresponding SAED pattern similar to Figure 3b, and therefore the chain axis (*c*-axis) is weakly but preferentially oriented in the vertical direction of this dark-field image.

also recognized. The width of fibrillar entities in Figures 1, 2, and 3a is measured to be about 10 nm, as indicated in Figure 3a for the specimen crystallized at 161 °C. This value might be regarded as the lamellar thickness but is not always reliable because the specimen for Figure 1 was metal-shadowed and the images of Figures 2 and 3a were taken at a fairly large amount of under-focus setting.[29,30] In fact, the lamellar thickness of i-PS crystallized isothermally at 160−170 °C was reported to be 12−14 nm.[8,12,31]

The crystal structure of i-PS was analyzed by Natta et al. (trigonal; a = 2.19 nm, c (chain axis) = 0.665 nm).[32,33] All the SAED patterns in this study (for example, Figure 3b) were well indexed with these unit cell constants. In Figure 3b, a pair of fairly sharp arc-shaped 300 reflections are observed on the equator (in Figure 3b, the "equator" is not horizontal but tilted), and weak 211 and $10\bar{2}$ reflections are visible off-meridionally and nearly on the meridian, respectively, as schematically illustrated in Figure 3c. (As indicated with the arrow showing the direction of the c*-axis in Figure 3b, the polymer chains are preferentially oriented from the lower left to the upper right in Figure 3a, probably due to some flow when the i-PS hot solution in *p*-xylene was spread on the hot water surface. To identify the directional relationship between a morphological image and its corresponding SAED pattern, such an oriented specimen film was utilized here.) No reflections attributed to the (110) or (220) planes are, however, recognized in Figure 3b though, for example, the absolute value of structure factor for the 220 reflection is much greater than that for 300.[33] The SAED pattern of Figure 3b, therefore, shows a tendency for the uniplanar axial orientation in which the *c*-axis (chain axis) and the (110) plane are parallel to the film surface. Each of the fibrillar entities in Figure 1 and the dark fibrillar striations in Figures 2 and 3a are, consequently, attributed to an edge-on (or nearly so) crystalline lamella. This orientation is also confirmed from the dark-field image taken by using a 300 reflection as shown in Figure 4. In Figure 3, a region in which edge-on lamellae are densely stacked seems to correspond to the location of row nucleation. These edge-on lamellae appear to grow from a row nucleus in both directions perpendicular to the flow direction, to splay gradually, and then to impinge upon lamellae grown from another

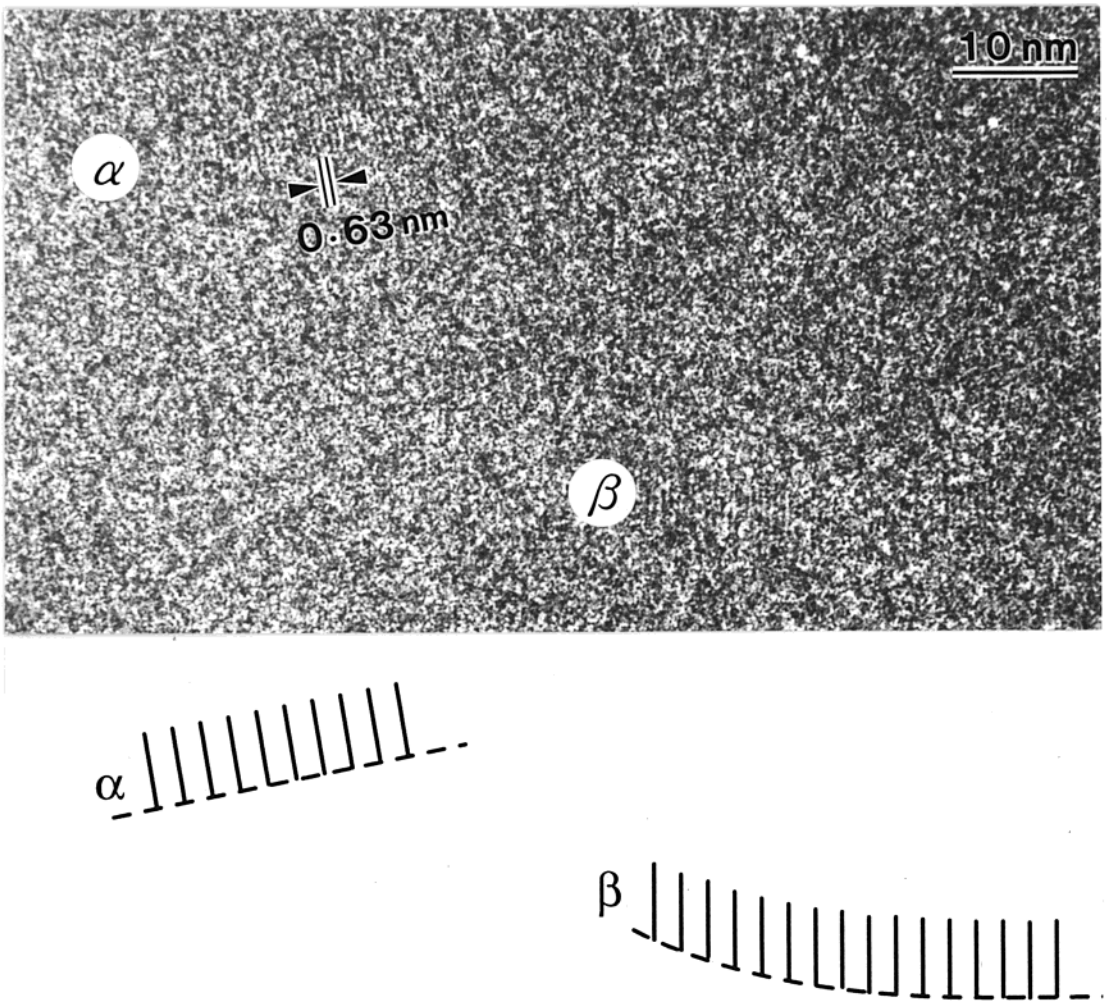

Figure 5. HRTEM image of edge-on lamellae in an i-PS thin film which was crystallized at 161 °C for 7 min. The schematic illustration at the bottom of the figure shows the location and direction of (300) lattice fringes in the HRTEM image.

row nucleus. Though seemingly branched striations are observed in some places of Figure 3, it is difficult to judge whether they impinged or were really branched.

Figure 4 shows an example of a dark-field image of an i-PS thin film annealed/crystallized at 161 °C for 7 min. This image was taken by using one of a pair of the arc-shaped 300 reflections. The SAED pattern obtained from this specimen film also showed preferential orientation as that from the specimen used for Figure 3, and most of the polymer chains are to be preferentially oriented in the vertical direction of Figure 4. In Figure 4, fine bright striations oriented in the horizontal direction are the regions which contribute to the 300 reflection utilized for dark-field imaging; that is to say, each of the bright striations corresponds to a crystalline region in a lamella. This dark-field image provides the conclusive evidence that the fibrillar entities recognized in the bright-field images (Figures 1, 2, and 3a) are edge-on (or nearly so) lamellar crystals of i-PS.[31] Thus, it is deduced that a crystalline lamella grows in the direction normal to the (300) plane and its growing face is the (300) plane. Furthermore, the width of these fine bright striations was measured to be 6−7 nm. The crystalline-core thickness of the i-PS lamellar crystal grown at 161 °C, therefore, can be estimated, and this value is 6−7 nm if such lamellae are standing strictly in the edge-on orientation. A finite orientational distribution of lamellae around the strict edge-on position, however, should be also taken into consideration. In Figure 4, it is unfortunately difficult to identify lamellar branching, though some edge-on lamellae are found to stack parallel side by side with each other.

3.2. High-Resolution TEM (HRTEM) Observation. The total end-point dose (TEPD), namely the electron dose necessary for complete disappearance of crystalline reflections in the SAED pattern, of i-PS crystal is around 2000 electrons nm^{-2} (approximately 0.03 Coulombs cm^{-2}) for 200 kV electrons at room temperature.[9,11] The lattice spacings of i-PS crystal, especially its (*hk*0) spacings, are invariant with increasing electron irradiation dose.[4] Owing to these facts, HRTEM observation of i-PS crystals can be realized even at room temperature.[3,4,9]

Figure 5 shows a HRTEM image of a thin film of i-PS, which was annealed/crystallized at 161 °C for 7 min. Lattice fringes with a spacing of 0.63 nm are identified in the image, which correspond to the (300) lattice planes of i-PS crystal. Slender regions, in which the lattice fringes are observable (for example, part α located at the upper left of and part β at the lower right of the image), are recognized. As schematically illustrated at the bottom of Figure 5, the slender region, part α, is almost a straight rectangle, but the other region, part β, is gradually curved. Each of the regions corresponds to an edge-on lamella, strictly speaking, to one crystallite (or the crystalline core of the lamella). Thus, the length of the (300) lattice fringes, namely the thickness of the crystalline core in an edge-on lamella

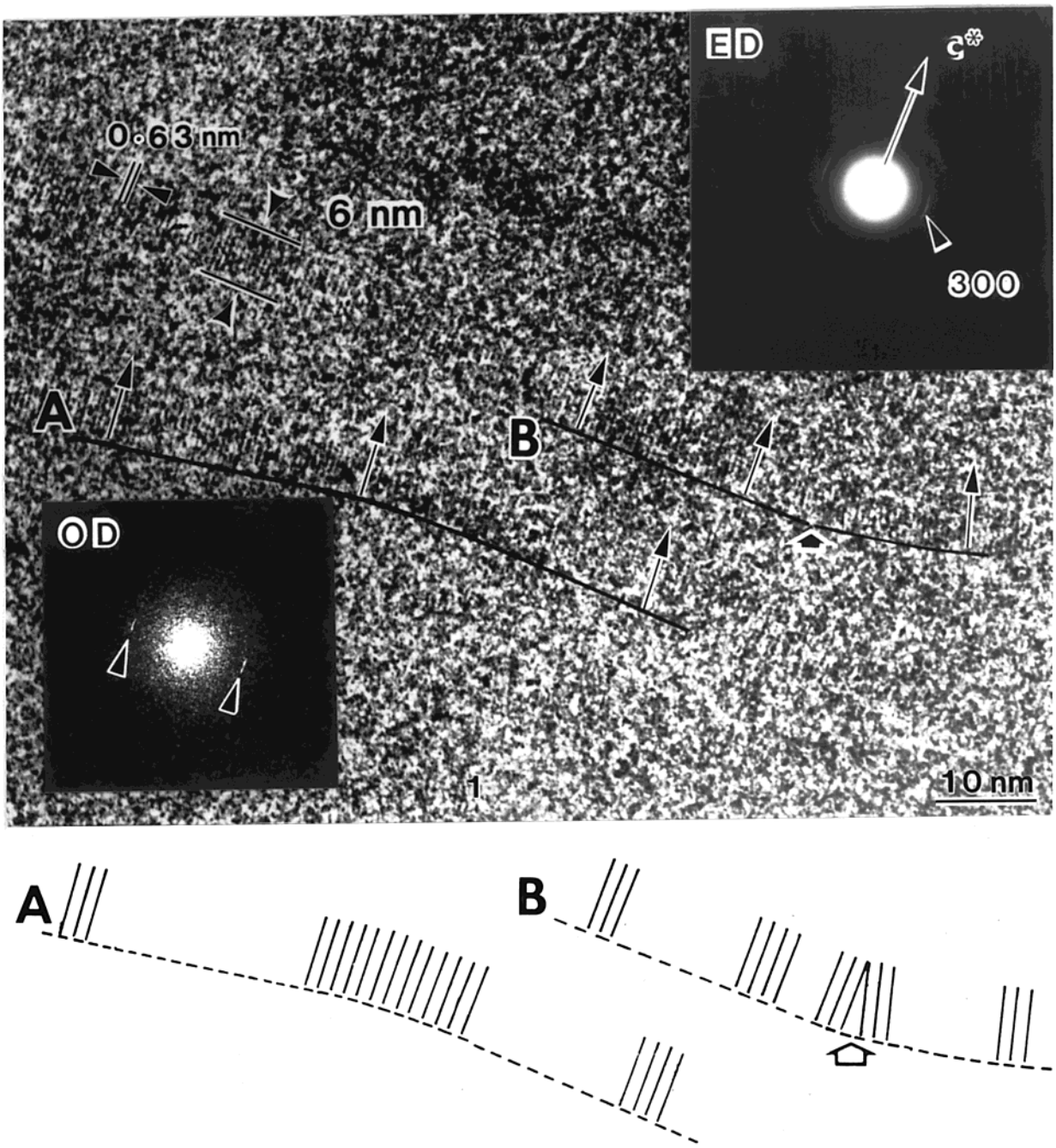

Figure 6. HRTEM image of curved edge-on lamellae in an i-PS thin film which was crystallized at 161 °C for 7 min. The insets, ED and OD, are respectively the SAED pattern obtained from the specimen film and the optical diffraction pattern obtained from the corresponding area in the original negative, which area includes the HRTEM image under consideration. The schematic illustration at the bottom of the figure shows the location and direction of (300) lattice fringes in the HRTEM image. The thick arrow in part B indicates the position of lamellar bending.

grown at 161 °C, is estimated at about 6 nm, though the image contrast of the fringes in Figure 5 is not sufficient.

Figure 6 shows another HRTEM image obtained from curved edge-on lamellae in a thin film of i-PS, which was annealed/crystallized at 161 °C for 7 min. The arrows in the image indicate the directions of the (300) lattice fringes, as schematically illustrated at the bottom of this figure. The inset, ED, in the figure is a SAED pattern from the specimen film, showing a pair of sharp reflection arcs of 300, and this SAED pattern is similar to that in Figure 3b. The other inset in Figure 6 is the optical diffraction (OD) pattern obtained from the corresponding area in the original negative, which area includes this HRTEM image under consideration. This OD pattern clearly shows a pair of sharp and short reflection arcs of 300, which indicate that there exists a restricted distribution of directions of the (300) fringes in the HRTEM image. Undoubtedly in the image, the direction of lattice fringes in part A is slightly different from that in part B.

The (300) lattice fringes in Figure 6 are more clearly observed than those in Figure 5. The length of the fringes, namely the crystalline-core thickness is certainly about 6 nm, as indicated in the figure. This value is, of course, is nearly compatible with that obtained from the dark-field observation of another specimen crystallized at 161 °C (e.g., 6−7 nm in Figure 4), because

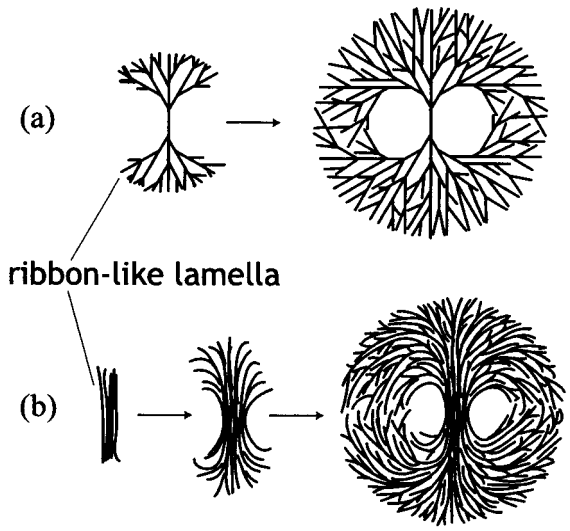

Figure 7. Two typical models of homogeneously nucleated spherulite of flexible-chain polymer, which are respectively comprised of (a) straight ribbonlike lamellae with branching[16] and (b) curved and splayed ribbonlike lamellae[19] which are grown plausibly by "spawning".[8] In these two-dimensional spherulites, the ribbonlike lamellae are in the "edge-on" orientation. The stage with a sheaflike appearance in (b), namely the illustration in the middle of (b), seems to correspond to a transitional hedrite stage.[17]

a similar region in an edge-on lamella, which region has given the 300 reflection in question, is visualized in both high-resolution and dark-field observations. Accordingly, there is no serious difference in estimation of crystallite size (viz., of crystalline-core thickness) between dark-field TEM and HRTEM. However, the crystalline-core thickness estimated from the lattice images is more precise and reliable than that obtained from dark-field observation only if the lamellae are strictly set in the "edge-on" position, because the (300) lattice fringes of 0.63 nm spacing can be utilized as an internal standard for magnification calibration.[9] In any event, it is noted that the crystalline-core thickness is considerably smaller than the coresponding lamellar thickness.[9,31] Furthermore, the contrast of HRTEM image is directly related to the arrangement of the molecular chains, that is to say, the direction of (300) lattice fringes indicates that of the chain stems in a crystallite, and consequently the shape and orientation of crystallites and the lattice defects if present in a crystallite can be visualized at the molecular level resolution. Figures 5 and 6 clearly reveal that there exist, at least, two microstructural features giving rise to the curvature of a lamella, and these might be associated with some deformation of lattice planes: (1) The lattice planes are aligned side by side but in a staggered (or longitudinally shifted) fashion (part β in Figure 5 and part A in Figure 6). (2) The neighboring crystallites in a lamella, in each of which the lattice planes are regularly aligned side by side with no staggering, are slightly but distinctly changed in orientation with each other (part B in Figure 6; the lamella appears to be "bent" at the position indicated with the thick arrow). The origin of this phenomenon is not known now, though a kind of crystallographic twinning might be one of the possibilities.

Figure 7a shows a model of polymer spherulite whose constituents are ribbonlike lamellae.[16] These ribbonlike lamellae branch frequently during their growth. Each of the lamellae is straight. However, by repeated branching for space filling (if the lamellae branch at a regular "branching angle", the branching in question is probably crystallographic branching, for example, like a dendritic mechanism (or a twinning one)[15,17]), they will grow into a sheaflike structure and finally into a spherulite leaving a binocular-like open space near the center. This type of spherulitic structure seems to be due to homogeneous nucleation in the polymer film.[15,19] Lamellar branching is recognized, for example in Figures 1 and 2, though it seems to occur infrequently. Figure 7b is a different model of polymer spherulite proposed by Phillips,[19] and similar models were also presented by other researchers.[17,18] This figure also shows a binocular-like open space due to homogeneous nucleation. In this model, however, ribbonlike lamellae are nucleated (probably by "spawning"[8]) one after another during spherulitic growth and are curved and splayed (or fanned) for space filling. The TEM study on i-PS thin films reported by Edwards and Phillips[8] has supported the "spawning" of new lamellar crystals, which means that a new lamellar crystal (or a daughter lamella) is nucleated just near the mother lamella probably as a result of chain entanglements in the polymer melt. This daughter lamella is likely to be parallel to the mother one. In the case of spawning, therefore, most of the constituent lamellae of a mature/immature spherulite and of a sheaflike structure, namely most of the spawned lamellar crystals, should be curved and splayed,[8] as illustrated in Figure 7b, and the curved profile of spawned lamellae might be attributted to a concentration gradient of crystallizable materials.[8] We note that most of the lamellae observed in Figures 1, 2, and 3a are really curved. Hence, the formation of curved lamellar crystals is one of the necessary conditions for spherulitic growth of a polymer such as i-PS, as shown in Figure 7b. Our HRTEM results clearly demonstrated the two manners for producing the curved lamellae.

Finally, it should be noted that the model illustrated in the middle of Figure 7b corresponds to a transitional hedrite stage.[17] This model resembles well, in appearance, the sheaflike structures observed here and there in Figure 2 and the one located at the lower left of Figure 1a, which are all, therefore, supposed to be hedrites.

4. Concluding Remarks

In this report, structural studies by TEM, in particular by HRTEM, of crystalline thin film of i-PS were presented. As for the space-filling mechanism of spherulitic growth, branching of straight lamellae was proposed previously as one of the possible mechanisms, as illustrated in Figure 7a. On the other hand, a different mechanism base on the "spawning" of new lamellae was subsequently proposed, as illustrated in Figure 7b. As described above, however, in this latter case most of the spawned lamellae of a mature/immature spherulite and of a sheaflike structure should be curved and splayed. From our results of morphological observation by TEM (for example, from Figures 1 and 2), it is deduced that both branching and spawning occur together in the process of spherulitic growth, because some lamellae are seemingly straight and branched but the other lamellae are really curved. However, for example, at (or near) the center of a spherulite or of a sheaflike structure, several lamellae are located side by side, and therefore spawning seems to be a principal mechanism of spheru-

litic growth in i-PS. In this study, we have succeeded to visualize, at the molecular level resolution by HR-TEM, the two manners (see the lattice fringes in part A and part B of Figure 6) for producing such curved lamellar crystals which are present with an edge-on orientation in crystalline thin films of i-PS. Repetition of one of these two manners or combination of them is to produce a curved ribbonlike edge-on lamella which is observed as a seemingly continuous striation in Figures 1, 2, and 3a.

Acknowledgment. M. Fujita expresses his thanks to the Research Fellowships of the Japan Society for the Promotion of Science (JSPS) for appointing him as a JSPS Research Fellow (1998−2001). This work was partly supported by a Grant-in-Aid for JSPS Fellows (No. 9796; to M. Fujita) and also partly by a Grant-in-Aid for Scientific Research on Priority Areas, "Mechanism of Polymer Crystallization" (No. 12127207; to M. Tsuji), both of which were from the Ministry of Education, Culture, Sports, Science and Technology of Japan.

References and Notes

(1) Blasis, B.; Manley, R. St. J. *J. Poym. Sci., Part A-2* **1966**, *4*, 1022.
(2) Lemstra, P. J.; Challa, G. J. *J. Polym. Sci., Polym. Phys. Ed.* **1975**, *13*, 1809.
(3) Tsuji, M.; Roy, S. K.; Manley, R. St. J. *Polymer* **1984**, *25*, 1573.
(4) Tsuji, M.; Roy, S. K.; Manley, R. St. J. *J. Polym. Sci., Polym. Phys. Ed.* **1985**, *23*, 1127.
(5) Tanzawa, Y. *Polymer* **1992**, *33*, 2659.
(6) Miyamoto, Y.; Tanzawa, Y.; Miyaji, H.; Kiho, H. *Polymer* **1992**, *33*, 2497.
(7) Li, Y.; Xue, G. *Macromolecules* **1999**, *32*, 3984.
(8) Edwards, B. C.; Phillips, P. J. *Polymer* **1974**, *15*, 351.
(9) Tsuji, M.; Uemura, A.; Ohara, M.; Kawaguchi, A.; Katayama, K.; Petermann, J. *Sen-i Gakkaishi* **1986**, *42*, T-580.
(10) Matsuba, G.; Kaji, K.; Nishida, K.; Kanaya, T.; Imai, M. *Polym. J.* (*Tokyo*) **1999**, *31*, 722.
(11) Shimizu, T.; Tsuji, M.; Kohjiya, S. *Sen'i Gakkaishi* **2001**, *57*, 137.
(12) Blais, J. J. B. P.; Manley, R. St. J. *J. Macromol. Sci., Phys.* **1967**, *B1*, 525.
(13) Izumi, K.; Ping, G.; Toda, A.; Miyaji, H.; Miyamoto, Y. *Jpn. J. Appl. Phys.* **1992**, *31*, 626.
(14) Hashimoto, M.; Amasaki, T.; Itoh, T. *Kobunshi Ronbunshu* **1999**, *56*, 821.
(15) Wunderlich, B. *Macromolecular Physics;* Academic: New York, 1973; Vol. 1.
(16) Okui, N. *Kobunshi no kesshou (Polymer Crystals)*; Kyoritsu: Tokyo, 1993; p 36.
(17) Khoury, F.; Passaglia, E. In *Treatise on Solid State Chemistry*; Hannay, N. B., Ed.; Plenum Press: New York, 1976; Vol. 3, Chapter 6, pp 335−496.
(18) Bassett, D. C. *Principles of Polymer Morphology*; Cambridge University Press: Cambridge, 1981.
(19) Phillips, P. J. In *Handbook of Crystal Growth*; Hurle, D. T. J., Ed.; North-Holland: Amsterdam, 1994; Vol. 2, Chapter 18, pp 1167−1216.
(20) Kobayashi, K. In *Kobunshi no bussei (Properties of polymers)*; Nakajima, A., Tadokoro, H., Tsuruta, T., Yuhki, H., Ohtsu, T., Eds.; Kagakudojin: Kyoto, 1964; Chapter 11, pp 203−220.
(21) Tsuji, M. In *Comprehensive Polymer Science*; Sir Allen, G., Bevington, J. C., Eds.; Pergamon: Oxford, 1989; Vol. 1, Chapter 34, pp 785−840.
(22) Yeh, G. S. Y.; Lambert, S. L. *J. Appl. Phys.* **1971**, *42*, 4614.
(23) Imai, M.; Mori, K.; Mizukami, T.; Kaji, K.; Kanaya, T. *Polymer* **1992**, *33*, 4451.
(24) Imai, M.; Mori, K.; Mizukami, T.; Kaji, K.; Kanaya, T. *Polymer* **1992**, *33*, 4457.
(25) Tsuji, M.; Kohjiya, S. *Prog. Polym. Sci.* **1995**, *20*, 259.
(26) Tosaka, M.; Yamakawa, M.; Tsuji, M.; Kohjiya, S.; Ogawa, T.; Isoda, S.; Kobayashi, T. *Microsc. Res. Tech.* **1999**, *46*, 325.
(27) Heidenreich, R. D. *Fundamentals of Transmission Electron Microscopy*; Interscience Publishers: New York, 1964.
(28) Petermann, J.; Gleiter, H. *Philos. Mag.* **1975**, *31*, 929.
(29) Christner, G. L.; Thomas, E. L. *J. Appl. Phys.* **1977**, *48*, 4063.
(30) Tsuji, M.; Manley, R. St. J. *Sen'i Gakkaishi* **1986**, *42*, T-323.
(31) Tsuji, M.; Uemura, A.; Ohara, M.; Isoda, S.; Kawaguchi, A.; Katayama, K. *Koenshu—Kyoto Daigaku Nippon Kagaku Sen'i Kenkyusho* **1987**, *44*, 1.
(32) Natta, G.; Corradini, P. *Makromol. Chem.* **1955**, *16*, 77.
(33) Natta, G.; Corradini, P.; Bassi, I. W. *Nuovo Cimento (Suppl.)* **1960**, *15*, 68.

MA010203N